

## THE INFLUENCE OF ACID TREATMENT ON THE COMPOSITION OF BENTONITE

ZORICA VUKOVIĆ<sup>1</sup>, ALEKSANDRA MILUTONOVIĆ<sup>1,\*</sup>, LJILJANA ROŽIĆ<sup>1</sup>, ALEKSANDRA ROSIĆ<sup>2</sup>, ZORAN NEDIĆ<sup>3</sup>  
AND DUŠAN JOVANOVIĆ<sup>1</sup>

<sup>1</sup> Institute of Chemistry, Technology and Metallurgy, Department of Catalysis and Chemical Engineering, Njegoševa 12, Belgrade, Republic of Serbia

<sup>2</sup> Faculty of Mining and Geology, Đušina 7, Belgrade, Republic of Serbia

<sup>3</sup> Faculty of Physical Chemistry, Studentski trg 12-16, 11000 Belgrade, Republic of Serbia

**Abstract**—Bentonite from the ‘Bogovina’ coal mine in Serbia, was characterized. The influence of acid treatment on its composition, as well as mathematical descriptions of this influence are reported. The purpose of this work was to correlate the concentration of the acid used for the treatment with the resulting bentonite composition. X-ray diffraction (XRD), infrared spectroscopy and quantitative chemical analysis were employed to define the changes caused by acid treatment.

The contents of all the cations, except Si, decreased exponentially with increasing concentration of the HCl used for the treatment of the bentonite. This approach was tested on previously published data and was shown to be valid.

The basal reflections of smectite decreased gradually and eventually disappeared after intense treatment, while the other reflections remained in the XRD patterns of all the samples, but decreased slightly with increasing acid strength. In addition, the amount of X-ray amorphous matter formed increased rapidly with increasing acid concentration up to 4.5 M. With further increase in the acid strength, the amount of X-ray amorphous matter remained virtually constant.

**Key Words**—Acid Treatment, Bentonite, Chemical Analysis, IR, XRD.

### INTRODUCTION

The physical, chemical and adsorption properties of natural bentonites depend on the crystal structure of their constituent clay minerals. Bentonites are rich in smectite, regardless of their mode of origin. In addition to smectite, bentonites also contain quartz, mica/illite, feldspar, calcite, carbonates, plagioclase, *etc.* (Komadel, 2003; Vaccari, 1998).

Natural bentonites usually do not exhibit sufficient adsorption and catalytic properties and, therefore, they have to be treated in order to enhance these properties. Acid activation of bentonites refers to the controlled, partial dissolution of the raw materials by mineral acids. Upon acid treatment, cations are leached from the octahedral and tetrahedral sheets, impurities such as calcite are dissolved, and exchangeable cations are replaced by hydrogen ions. Simultaneously, the edges of platelets open. All these changes result in an increase in the specific surface area and pore volume of the clays (Christidis *et al.*, 1997; Falaras *et al.*, 1999; Jovanović *et al.*, 1996; Valenzuela-Díaz and Santos, 2001; Vuković *et al.*, 2005).

Thus, acid treatment is commonly required when bentonites are used in industry, *e.g.* in beer stabilization, in the pharmaceutical industry and as catalysts and catalyst support in different processes. One of the most

common applications of acid-treated bentonite is as bleaching clays, *i.e.* they are used to remove color, odor and other impurities from edible vegetable and animal oils or mineral and petroleum oils (Christidis *et al.*, 1997; Falaras *et al.*, 1999; Valenzuela-Díaz and Santos, 2001).

Although acid treatment of bentonites originating from different localities worldwide has been studied extensively (Christidis *et al.*, 1997; Falaras *et al.*, 1999; Jovanović *et al.*, 1996; Mendioroz *et al.*, 1987; Novak and Čičel, 1978; Valenzuela-Díaz and Santos, 2001; Vuković *et al.*, 2005), this paper presents some aspects that have not been studied previously. The investigation was performed on raw clay material from the coal mine known as ‘Bogovina’ in Serbia which has only been partially described (Vuković *et al.*, 2005). The influence of acid treatment of this clay is presented, along with a new approach for the quantification of the influence of the acid treatment. The goal was to determine the mathematical equations which best describe the influence of acid strength on the change in composition of bentonite. The results of the chemical analyses were fitted with different mathematical functions in order to find the most appropriate ones. The XRD and infrared (IR) results were used to show trends of phase changes induced by increasing the applied acid concentration.

### MATERIALS AND METHODS

A sample of bentonite with the largest smectite content from the area of Bogovina was selected for further investigation. The chemical composition (wt.%) of the

\* E-mail address of corresponding author:  
snikolic@nanosys.ihtm.bg.ac.yu  
DOI: 10.1346/CCMN.2006.0540605

selected sample, dried at 110°C, is: SiO<sub>2</sub> 57.51, Al<sub>2</sub>O<sub>3</sub> 17.13, Fe<sub>2</sub>O<sub>3</sub> 7.67, MgO 2.35, CaO 1.81, Na<sub>2</sub>O 0.75, K<sub>2</sub>O 1.18 and CO<sub>2</sub> 0.5. The loss on ignition was 11.10 wt.%.

The raw material was ground to pass through a 74 µm sieve. This size was chosen for acid treatment because the acid-treated bentonites employed in oil-bleaching processes are of this size (Valenzuela Diaz and Santos, 2001).

The samples were treated chemically with solutions of HCl of nominal concentrations: 1.5, 3.0, 4.5, 6.0 and 7.5 mol dm<sup>-3</sup>. The mass ratio of the acid solution and the clay was 4:1. Treatment of the bentonite samples was carried out at 90°C for 2 h. The suspension was filtered through a Buchner funnel while hot. The filtration cake was rinsed with hot distilled water until the filtrate was Cl<sup>-</sup> and/or Fe<sup>3+</sup> free (tested with AgNO<sub>3</sub> and K<sub>3</sub>[Fe(CN)<sub>6</sub>], respectively).

A Philips PW 1710 X-ray powder diffractometer with a Cu anticathode ( $\lambda = 0.154178$  nm) operating at 40 kV and 30 mA was used to monitor the structural changes caused by the chemical treatment.

Chemical analysis of the bentonites was performed and used to examine the effect of acid treatment on the composition of the treated bentonites. The amount of SiO<sub>2</sub> was determined by the classical gravimetric method. After removal of the silica using a mixture of HF and H<sub>2</sub>SO<sub>4</sub> and heating, an atomic absorption spectrophotometer (AAS) with an air-acetylene flame was used to estimate the contents of K<sup>+</sup>, Na<sup>+</sup> and Fe<sup>3+</sup>. In order to determine the amounts of Al<sup>3+</sup>, Ca<sup>2+</sup> and Mg<sup>2+</sup>, the AAS was run with a N<sub>2</sub>O-acetylene flame using samples that had previously been prepared by fusion in a mixture of Na<sub>2</sub>CO<sub>3</sub> and K<sub>2</sub>CO<sub>3</sub>.

The IR spectra were obtained using a Perkin-Elmer 983 G IR-spectrometer in the spectral range 4000–250 cm<sup>-1</sup>. The KBr pressed disc technique (2 mg of sample and 200 mg of KBr) was used.

## RESULTS AND DISCUSSION

Acid activation caused significant changes in the chemical composition of the bentonite. The relative SiO<sub>2</sub> content increased with increasing acid concentration, while that of all the other cations decreased (Figure 1). The cation oxide content presented in Figure 1 was calculated after subtracting the losses on ignition followed by normalization to 100 wt.% (Gates *et al.*, 2002).

The Na<sub>2</sub>O and CaO contents decreased sharply at small acid concentrations (1.5 mol dm<sup>-3</sup>). The mechanism of leaching Al<sub>2</sub>O<sub>3</sub>, Fe<sub>2</sub>O<sub>3</sub>, MgO and K<sub>2</sub>O followed a different trend. For these oxides, the leaching increased gradually with increasing HCl concentration. The influence of acid concentration on the changes in the chemical composition of the treated samples was evaluated and the corresponding equations for each oxide are given in Table 1. Different regression and

exponential functions were investigated and the equations with the best 'goodness of fit' values were chosen. The increase in the SiO<sub>2</sub> content with increasing HCl strength can be fitted by a second-degree polynomial, while all other oxides display an exponential decrease with increasing HCl concentration.

The exponential correlation of the cation content with acid concentration was also tested on previously published data (Falaras *et al.*, 1999) and yielded similar results (Table 2). It should be pointed out that in that case, although the activation was performed with another type of bentonite (Texas smectite) and a different mineral acid (H<sub>2</sub>SO<sub>4</sub>), similar behavior was observed.

The presence of Ca, Na and K in all samples, even those treated with the strongest acid concentrations, suggests that these cations originated from phases other than smectite, probably feldspar. Therefore, the equations presented in Tables 1 and 2 would have been different if pure smectite had been used.

The results shown in Tables 1 and 2 indicate that although the parameters in the equations vary depending on the chemical composition of the raw clay investigated, the type of oxide and the type of acid used for activation, the contents of all oxides which decrease with increasing acid strength do so in an exponential manner.

The XRD patterns of the raw bentonite and the acid-treated samples are presented in Figure 2. The raw clay consists of smectite, quartz, illite, calcite, feldspar and a

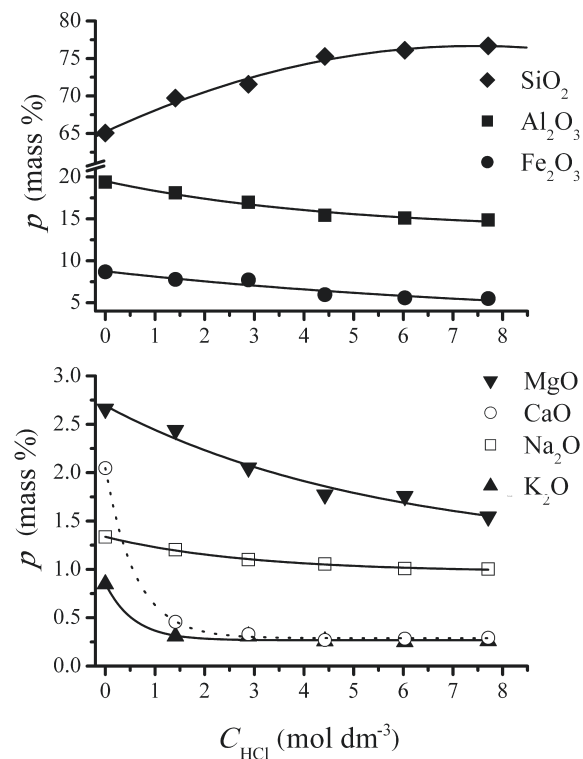


Figure 1. Dependence of the cation oxide contents in acid-treated samples on the HCl concentration employed.

Table 1. Dependence of the contents of oxides in the investigated samples on the applied HCl concentration.

| Oxide                          | Function   | Goodness of fit |
|--------------------------------|--|-----------------|
| SiO <sub>2</sub>               | $p_{\text{SiO}_2} = 65.22 + 3.068 \cdot C_{\text{HCl}} - 0.206 \cdot C_{\text{HCl}}^2$ | 0.9938          |
| Al <sub>2</sub> O <sub>3</sub> | $p_{\text{Al}_2\text{O}_3} = 13.619 + 5.871e^{-\frac{C_{\text{HCl}}}{4.448}}$          | 0.9923          |
| Fe <sub>2</sub> O <sub>3</sub> | $p_{\text{Fe}_2\text{O}_3} = 4.474 + 4.278e^{-\frac{C_{\text{HCl}}}{4.836}}$           | 0.9919          |
| MgO                            | $p_{\text{MgO}} = 1.192 + 1.500e^{-\frac{C_{\text{HCl}}}{5.416}}$                      | 0.9881          |
| CaO                            | $p_{\text{CaO}} = 0.289 + 1.759e^{-\frac{C_{\text{HCl}}}{0.609}}$                      | 0.9997          |
| Na <sub>2</sub> O              | $p_{\text{Na}_2\text{O}} = 0.266 + 0.582e^{-\frac{C_{\text{HCl}}}{0.568}}$             | 0.9966          |
| K <sub>2</sub> O               | $p_{\text{K}_2\text{O}} = 0.973 + 0.364e^{-\frac{C_{\text{HCl}}}{2.811}}$              | 0.9982          |

small amount of X-ray amorphous material. As expected, the calcite was removed during acid activation.

The influence of acid treatment on smectite can be observed by comparison of the intensity of the diffraction peaks of the original and the treated smectites. The intensity of diffraction peaks corresponding to smectite decrease with increasing acid strength. The treatment affected mainly the 001 reflections. In the present study, the 001 maximum disappeared after intense treatment with 4.5 M HCl. The prismatic *hk0* and other pinacoidal *0k0* reflections were slightly affected. Moreover, a hump

appeared between 19 and 30°2θ, which is attributed to X-ray amorphous matter. The area of this hump increased with increasing acid concentration.

The effects of acid treatment on the XRD patterns are summarized in Figure 3. The change in the intensity of the 001 smectite peak (expressed as the integral area) is given in Figure 3, curve 1.

The influence of acid treatment on the intensity of the smectite peak (110, 020 reflections) is shown in Figure 3, curve 2. The intensity was calculated as the area of the peak at 19.5–20.5°2θ, excluding the area of the amorphous matter. Curve 2 in Figure 3 shows that

Table 2. Dependence of the contents of oxides of previously published data (Falaras *et al.*, 1999) on the applied H<sub>2</sub>SO<sub>4</sub> concentration

| Type of oxide                  | Function   | Goodness of fit |
|--------------------------------|--|-----------------|
| SiO <sub>2</sub>               | $p_{\text{SiO}_2} = 76.88 + 1.570 \cdot C_{\text{HCl}} - 0.101 \cdot C_{\text{HCl}}^2$ | 0.9863          |
| Al <sub>2</sub> O <sub>3</sub> | $p_{\text{Al}_2\text{O}_3} = 11.556 + 5.260e^{-\frac{C_{\text{HCl}}}{5.784}}$          | 0.9906          |
| Fe <sub>2</sub> O <sub>3</sub> | $p_{\text{Fe}_2\text{O}_3} = 0.460 + 0.351e^{-\frac{C_{\text{HCl}}}{5.201}}$           | 0.9978          |
| MgO                            | $p_{\text{MgO}} = 2.794 + 1.076e^{-\frac{C_{\text{HCl}}}{0.505}}$                      | 0.9516          |
| CaO                            | $p_{\text{CaO}} = 0.735 + 1.135e^{-\frac{C_{\text{HCl}}}{0.184}}$                      | 0.9887          |
| K <sub>2</sub> O               | $p_{\text{K}_2\text{O}} = 0.045 + 0.055e^{-\frac{C_{\text{HCl}}}{0.419}}$              | 0.9094          |

acid treatment with higher concentrations of HCl (4.5–7.5 M) resulted in a greater decrease in the intensity of this band.

The X-ray amorphous matter was estimated from the integral area of the diffuse hump between 19 and 30°2 $\theta$ . The area was calculated after subtraction of the peaks corresponding to quartz at 26.7 and 20.9°2 $\theta$ , smectite at 19.9°2 $\theta$ , feldspar at 27.6°2 $\theta$  and calcite at 29.5°2 $\theta$ . The data used for the subtraction of background was provided by software supplied with the XRD instrument used for the experiment. As can be seen from Figure 3, curve 3, the amount of X-ray amorphous matter increases with increasing acid concentration up to 4.5 M HCl, after which it remains almost constant.

The IR spectra (Figure 4) confirmed the results of the XRD analysis, *i.e.* smectite was the dominant mineral phase (Breen *et al.*, 1997; Christidis *et al.*, 1997; Falaras *et al.*, 1999; Komadel *et al.*, 1996; Madejová *et al.*, 1998; Obut and Girgin, 2002; Temujin *et al.*, 2004). The broad band at 1430 cm<sup>-1</sup> in the spectrum of the raw clay, which is absent in the spectra of the treated samples, is assigned to a calcite impurity (Komadel *et al.*, 1996; Temujin *et al.*, 2004). The sharp band at 799 cm<sup>-1</sup>, with an inflection near 777 cm<sup>-1</sup>, confirms that the quartz admixture remained in all the samples (Falaras *et al.*, 1999; Madejová *et al.*, 1998).

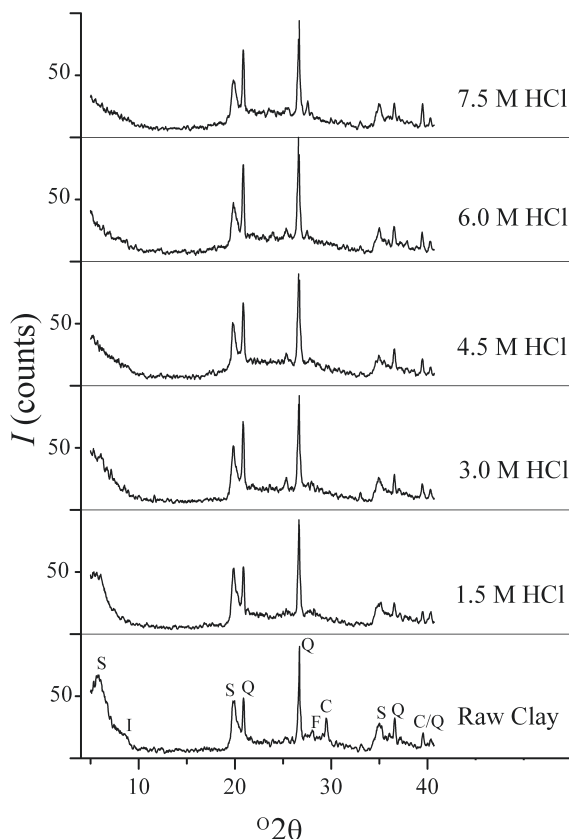


Figure 2. XRD patterns of the raw and acid-treated bentonites (S = smectite, Q = quartz, C = calcite, F = feldspar, I = illite).

The acid treatment affects the IR spectra as certain bands corresponding to the smectite structure decrease and shift. The broad complex band in the OH-stretching region around 3600 cm<sup>-1</sup> is characteristic of smectite and reflects a variety of environments of the hydroxyl groups (AlAlOH, AlMgOH, AlFeOH, FeMgOH and FeFeOH). The smaller values of the OH-stretching bands correspond to the cation pairs AlFe, FeMg and FeFe (3587–3532 cm<sup>-1</sup>), while the larger values (3684–3604 cm<sup>-1</sup>) correspond to AlAl and AlMg (Madejová *et al.*, 1994). No deconvolution of this OH-stretching band was performed. Therefore, it is not possible to state unambiguously which cation pairs contribute to this band, which decreased in magnitude and shifted from 3609 cm<sup>-1</sup> for the raw clay to 3621 cm<sup>-1</sup> for the acid-treated samples. This result indicates that the dissolution of Mg and Fe was more significant than that of Al.

The dissolution of the octahedral sheets caused by acid treatment can be followed by the intensity decrease of the band corresponding to OH-bending vibrations at ~910 cm<sup>-1</sup> (AlAlOH), the complete disappearance of the band at 860 cm<sup>-1</sup>, assigned to AlFeOH, as well as the diminution and disappearance of the band at 820 cm<sup>-1</sup>, assigned to FeFeOH bending vibrations (Breen *et al.*, 1997; Christidis *et al.*, 1997; Falaras *et al.*, 1999; Madejová *et al.*, 1998; Obut and Girgin, 2002; Temujin *et al.*, 2004).

The intensity of the band at 520 cm<sup>-1</sup>, attributed to Si–O–Al, decreased only for the samples treated with very high concentrations of HCl. This indicates that the dissolution of Al<sup>3+</sup> only becomes significant during the more intensive treatments (Breen *et al.*, 1997; Falaras *et al.*, 1999; Madejová *et al.*, 1998).

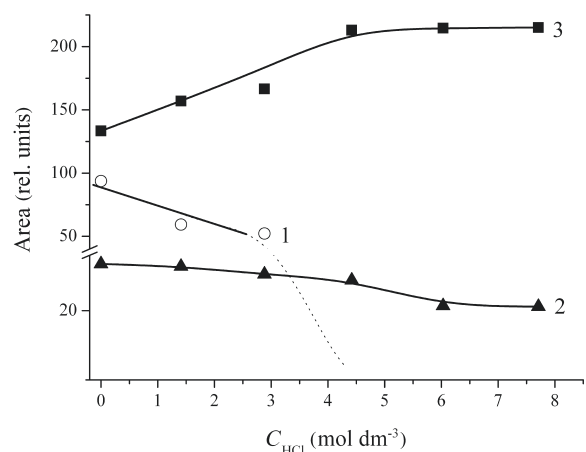


Figure 3. The influence of HCl concentration on XRD data: curve 1 – area under the peak corresponding to the 001 reflection of smectite; curve 2 – area under the smectite band corresponding to the 110, 020 reflections; and curve 3 – area under the diffuse peak corresponding to X-ray amorphous matter.

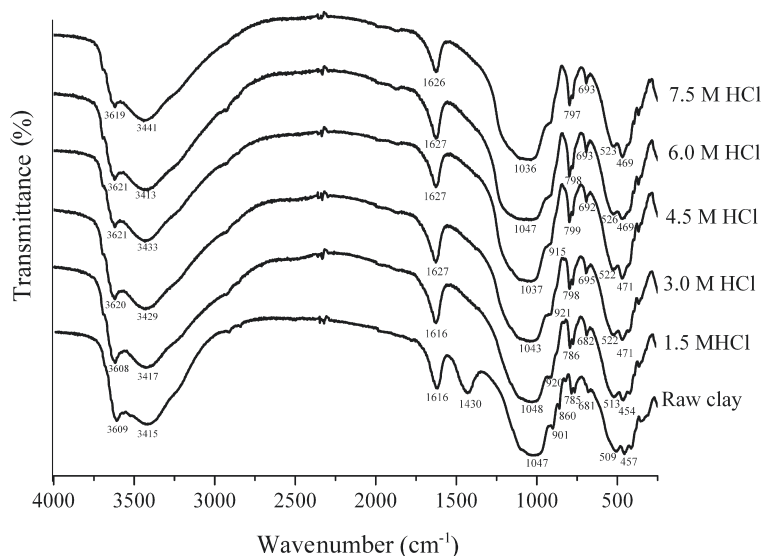


Figure 4. IR spectra of the raw and acid-treated bentonites.

Although the intensity of the Si–O stretching band near  $1045\text{ cm}^{-1}$  remained essentially unchanged (Christidis *et al.*, 1997), its shape changed due to the change in the Si–O environment from two-dimensional layers to three-dimensional X-ray amorphous silica. The increase in the intensity of the band near  $460\text{ cm}^{-1}$  also confirms an increase in the formation of X-ray amorphous silica (Christidis *et al.*, 1997), caused by increasing HCl strength. Both the IR and XRD analyses indicate that the amount of amorphous silica increases more rapidly with increasing HCl concentration up to 4.5 M HCl than it does with further increase in the HCl concentration.

The IR bands corresponding to various bonds in the smectite of the raw bentonite are shifted compared to literature data, whereas the bands in the acid-treated samples are comparable to those reported in the literature (Breen *et al.*, 1997; Christidis *et al.*, 1997; Falaras *et al.*, 1999; Madejová *et al.*, 1998; Obut and Girgin, 2002; Temuujin *et al.*, 2004).

## CONCLUSIONS

The changes in the chemical composition of bentonite from Bogovina after activation with HCl were quantified. The increase in the  $\text{SiO}_2$  content with increasing acid strength can be fitted by a second degree polynomial, while all other oxides display an exponential decrease with increasing concentration. This approach was tested on previously published data obtained for smectites of different origins, having a different composition and activated with a different mineral acid ( $\text{H}_2\text{SO}_4$ ), and was proven to be valid. It has been shown that although the parameters in the exponential equations vary and depend on the chemical composition of the investigated raw clay, the type of

oxide and the type of acid employed for activation, the content of all oxides which decrease with increasing acid strength do so in an exponential manner.

The most significant modifications were observed after acid treatment with 4.5 M HCl. The various IR bands of smectite in the raw bentonite were shifted compared to literature data, while the bands in the acid-treated samples were similar.

## ACKNOWLEDGMENTS

This work was supported by the Ministry of Science & Environmental Protection of the Republic of Serbia.

## REFERENCES

- Breen, C., Zahoor, F.D., Madejová, J. and Komadel, P. (1997) Characterization and catalytic activity of acid-treated, size-fractionated smectites. *The Journal of Physical Chemistry B*, **101**, 5324–5331.
- Christidis, G.E., Scott, P.W. and Dunham, A.C. (1997) Acid activation and bleaching capacity of bentonites from the islands of Milos and Chios, Aegean, Greece. *Applied Clay Science*, **12**, 329–347.
- Falaras, P., Kovanis, I., Lezou, F. and Seiragakis, G. (1999) Cotton seed oil bleaching by acid-activated montmorillonite. *Clay Minerals*, **34**, 221–232.
- Gates, W.P., Anderson, J.S., Raven, M.D. and Churchman, G.J. (2002) Mineralogy of a bentonite from Miles, Queensland, Australia, and characterisation of its acid activation products. *Applied Clay Science*, **20**, 189–197.
- Jovanović, N., Brezovska, S., Burevski, D., Boevska, V., Panova, B. and Vuković, Z. (1996) The effect of inorganic acids on the adsorption properties of bentonite. *Journal of the Serbian Chemical Society*, **61**, 453–460.
- Komadel, P. (2003) Chemically modified smectites. *Clay Minerals*, **38**, 127–138.
- Komadel, P., Bujdák, J., Madejová, J., Šuchá, V. and Elsass, F. (1996) Effect of non-swelling layers on the dissolution of reduced-charge montmorillonite in hydrochloric acid. *Clay Minerals*, **31**, 333–345.
- Madejová, J., Komadel, P. and Čičel, B. (1994) Infrared study

- of octahedral site populations in smectites. *Clay Minerals*, **29**, 319–326.
- Madejová, J., Bujdák, J., Janek, M. and Komadel, P. (1998) Comparative FT-IR study of the structural modifications during acid treatment of dioctahedral smectites and hectorite. *Spectrochimica Acta A*, **54**, 1397–1406.
- Mendioroz, S., Pajares, J.A., Benito, I., Pesquera, C., Gonzales, F. and Blanco, C. (1987) Texture evolution of montmorillonite under progressive acid treatment: change from H3 to H2 type of hysteresis. *Langmuir*, **3**, 676–681.
- Novak, I. and Čičel, B. (1978) Dissolution of smectites in hydrochloric acid: II. Dissolution rates as a function of crystallochemical composition. *Clays and Clay Minerals*, **26**, 341–344.
- Obut, A. and Girgin, I. (2002) The improvement of gelling property of bentonites using their physico-chemical and mineralogical characteristics. *Yerbilimleri*, **25**, 1–10.
- Temuujin, J., Jadambaa, Ts., Burmaa, G., Erdenechimeg, Sh., Amarasanaa, J. and MacKenzie, K.J.D. (2004) Characterisation of acid activated montmorillonite clay from Tuulant (Mongolia). *Ceramics International*, **30**, 251–255.
- Vaccari, A. (1998) Preparation and catalytic properties of cationic and anionic clays. *Catalysis Today*, **41**, 53–71.
- Valenzuela Diaz, F.R. and Santos, P.S. (2001) Studies on the acid activation of Brazilian smectitic clays. *Quimica Nova*, **24**, 345–353.
- Vuković, Z., Milutinović-Nikolić, A., Krstić, J., Abu-Rabi, A., Novaković, T. and Jovanović, D. (2005) The influence of acid treatment on the nanostructure and textural properties of bentonite clays. *Materials Science Forum*, **494**, 339–344.

(Received 17 August 2005; revised 7 June 2006; Ms. 1085; A.E. Peter Komadel)